Magnetism

Mean field theory

$$M = M_S \tanh\left(\frac{T_c}{T}\frac{M}{M_s}\right)$$

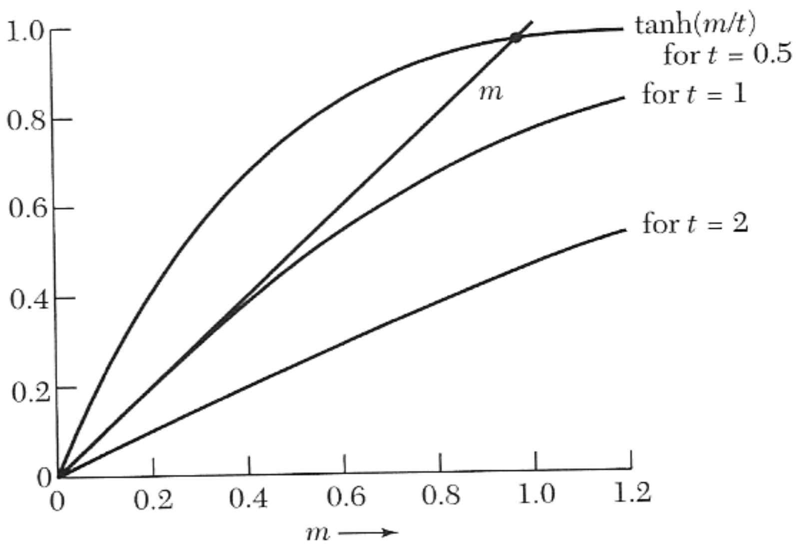

$$m = \tanh\left(\frac{m}{t}\right)$$

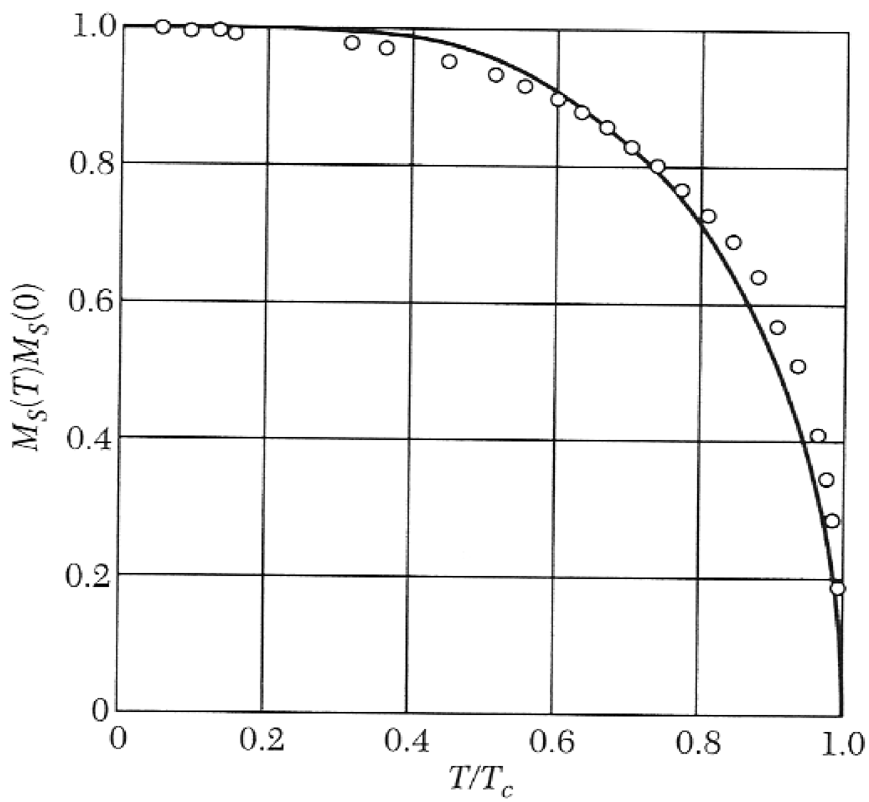

Experimental points for Ni.

$$M_S = \frac{N}{2V} g\mu_B \quad \text{and} \quad T_c = \frac{z}{4k_B} J$$

Source: Kittel

Ferromagnetism

Material	Curie temp. (K)	
Co	1388	
Fe	1043	
$FeOFe_2O_3$	858	
$NiOFe_2O_3$	858	
$CuOFe_2O_3$	728	
$MgOFe_2O_3$	713	
MnBi	630	
Ni	627	
MnSb	587	
$MnOFe_2O_3$	573	
$Y_3Fe_5O_{12}$	560	
CrO_2	386	
MnAs	318	
Gd	292	
Dy	88	
EuO	69	Electrical insulator
$Nd_2Fe_{14}B$	353	$M_s = 10\, M_s$(Fe)
Sm_2Co_{17}	700	rare earth magnets

$$M_S = \frac{N}{2V} g \mu_B$$

$$T_c = \frac{z}{4k_B} J$$

Curie - Weiss law

$$M = \frac{1}{2} g \mu_B \frac{N}{V} \tanh\left(\frac{g \mu_B \left(B_{MF} + B_a \right)}{2 k_B T} \right)$$

$$\vec{B}_{MF} = \frac{V}{N g^2 \mu_B^2} zJ\vec{M}$$

Above T_c we can expand the hyperbolic tangent $\tanh(x) \approx x$ for $x << 1$

$$M \approx \frac{1}{4} g^2 \mu_B^2 \frac{N}{V k_B T} \left(\frac{V}{N g^2 \mu_B^2} zJM + B_a \right)$$

Solve for M

$$M \approx \frac{g^2 \mu_B^2 N}{4 V k_B} \frac{B_a}{T - T_c}$$

$$T_c = \frac{z}{4 k_B} J$$

Curie Weiss Law $\chi = \frac{dM}{dH} \approx \frac{C}{T - T_c}$

Critical fluctuations near T_c

Ferromagnets are paramagnetic above T_c

Source: Kittel

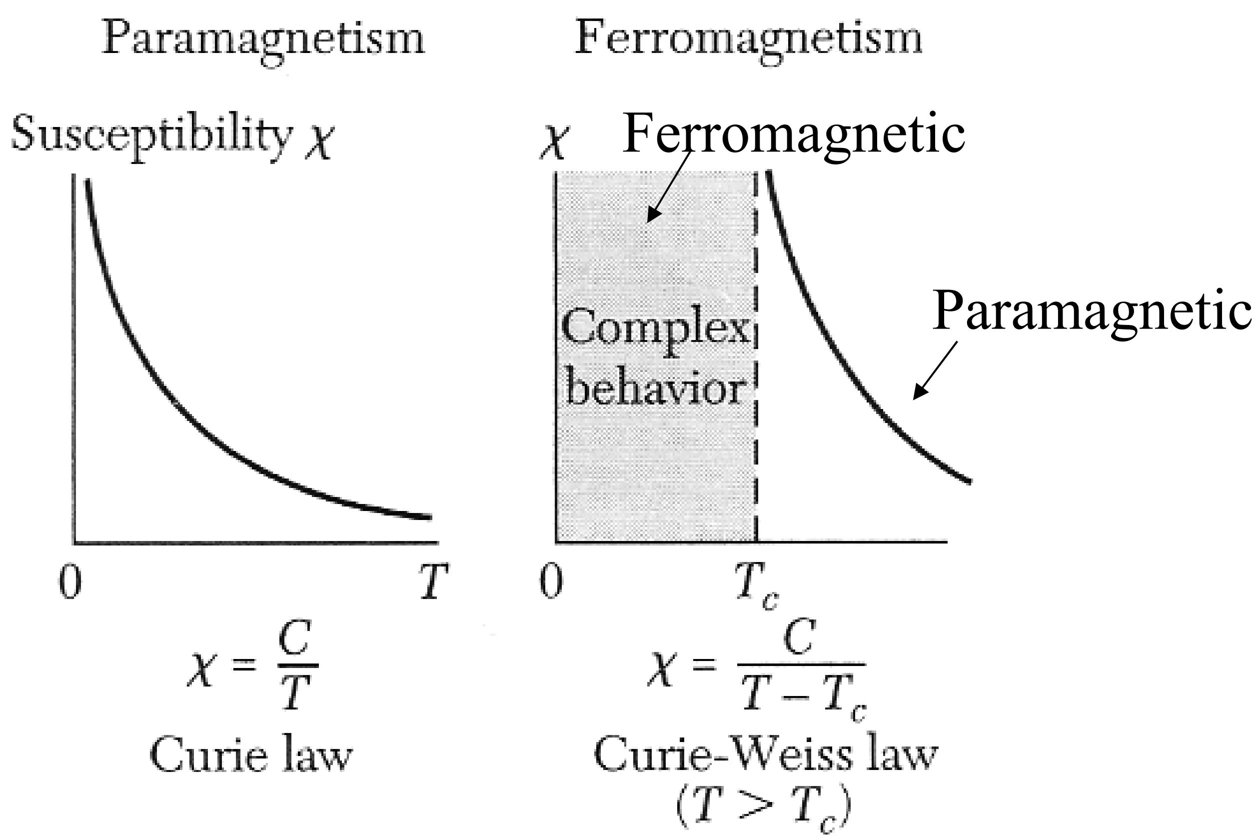

Critical fluctuations near T_c.

Magnetization of a Magnetite Single Crystal Near the Curie Point*

D. O. SMITH†
Laboratory for Insulation Research, Massachusetts, Institute of Technology, Cambridge, Massachusetts
(Received January 20, 1956)

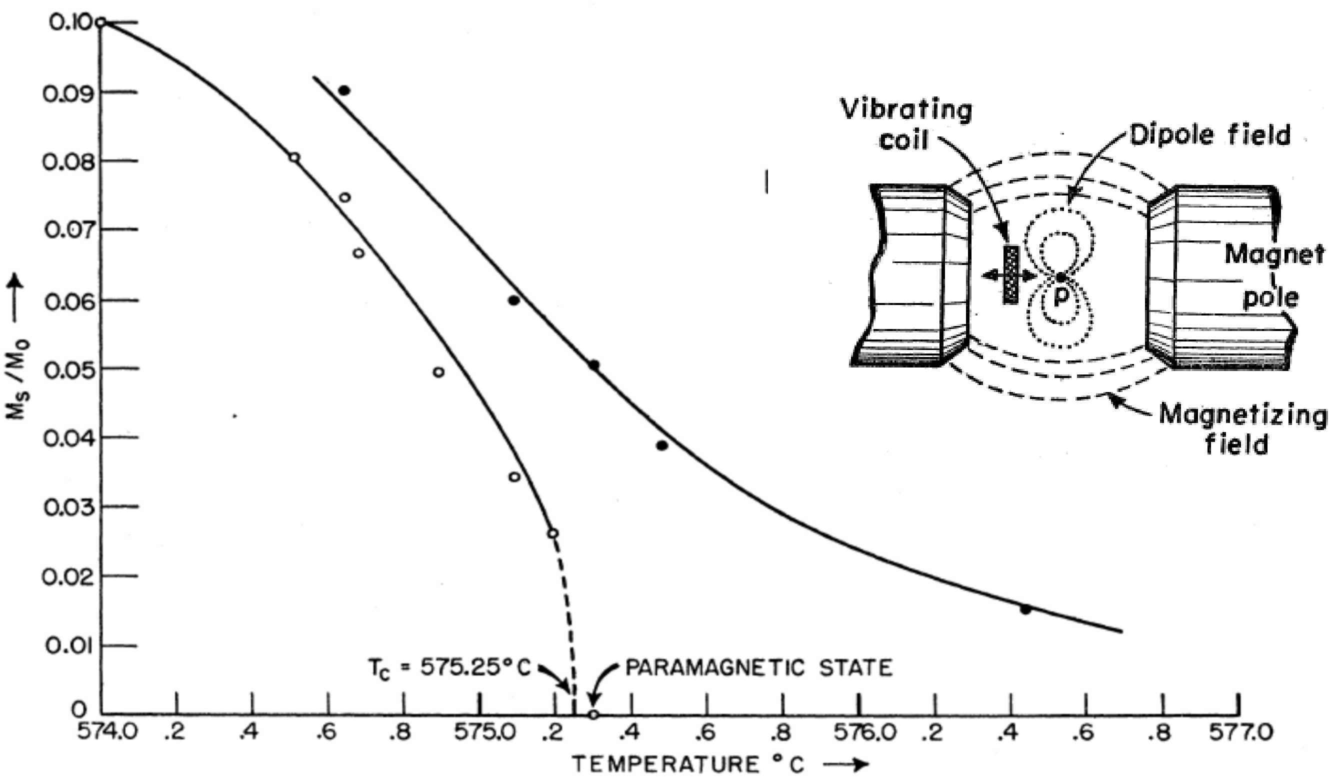

FIG. 9. M_s/M_0 *vs* T in the [111] direction near the Curie point for single-crystal magnetite.

FIG. 2. Principle of the vibrating-coil magnetometer.

Magnetic ordering

Ferromagnetism

Ferrimagnetism

Antiferromagnetism

Helimagnetism

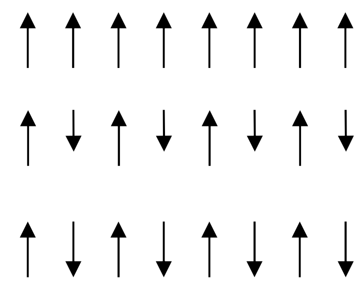

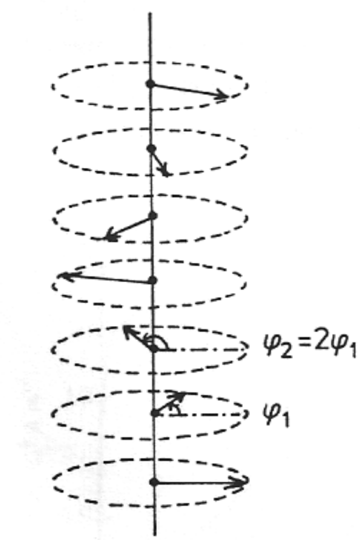

All ordered magnetic states have excitations called magnons

Ferrimagnets

Magnetite Fe_3O_4
(Magneteisen)

Ferrites $MO \cdot Fe_2O_3$

M = Fe, Zn, Cd, Ni, Cu,
Co, Mg

$\uparrow \downarrow \uparrow \downarrow \uparrow \downarrow \uparrow \downarrow$

Two sublattices A and B.

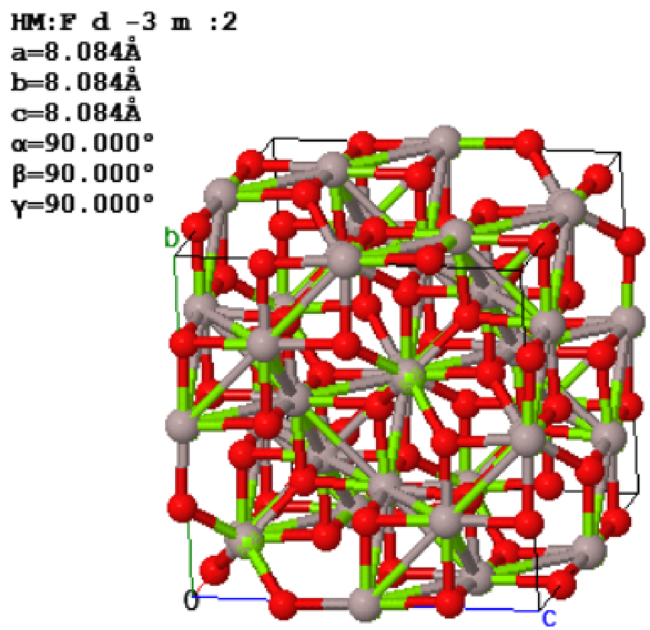

$MgAl_2O_4$

Spinel crystal structure XY_2O_4

8 tetrahedral sites A (surrounded by 4 O) $5\mu_B \uparrow$

16 octahedral sites B (surrounded by 6 O) $9\mu_B \downarrow$

per unit cell

Ferrimagnets

Magnetite Fe_3O_4

Ferrites $MO{\cdot}Fe_2O_3$

M = Fe, Zn, Cd, Ni, Cu, Co, Mg

$\uparrow \downarrow \uparrow \downarrow \uparrow \downarrow \uparrow \downarrow$

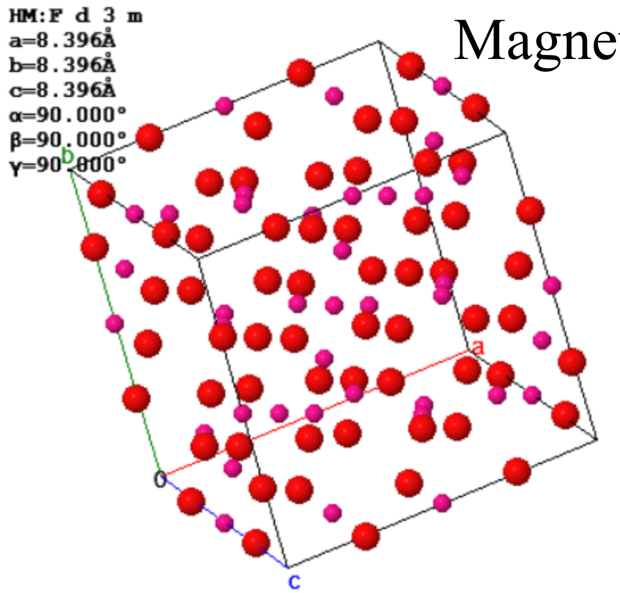

Magnetite

Exchange integrals J_{AA}, J_{AB}, and J_{BB} are all negative (antiparallel preferred)

$|J_{AB}| > |J_{AA}|,|J_{BB}|$

↑ ↓ ↑ ↓ ↑ ↓ ↑ ↓ Ferrimagnetism

gauss = 10^{-4} T
oersted = $10^{-4}/4\pi\times10^{-7}$ A/m

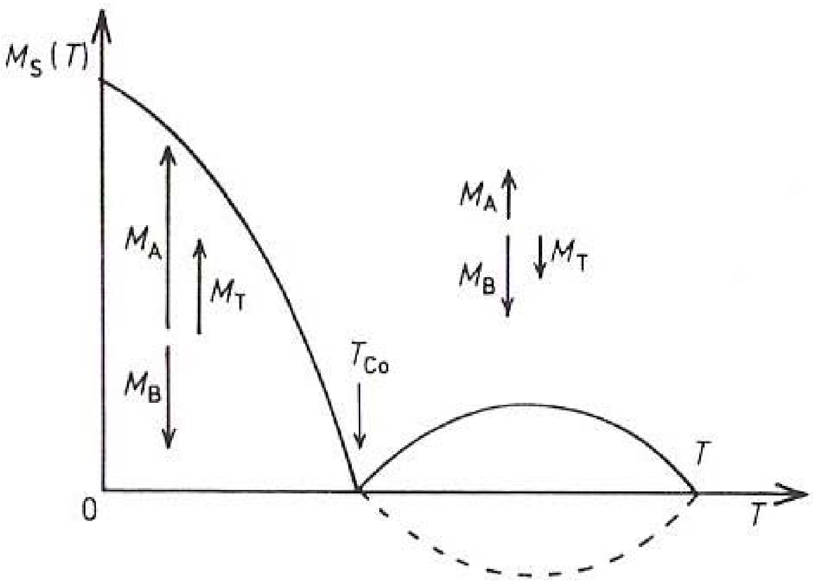

Table 33.3
SELECTED FERRIMAGNETS, WITH CRITICAL TEMPERATURES T_c AND SATURATION MAGNETIZATION M_0

MATERIAL	T_c (K)	M_0 (gauss)[a]
Fe_3O_4 (magnetite)	858	510
$CoFe_2O_4$	793	475
$NiFe_2O_4$	858	300
$CuFe_2O_4$	728	160
$MnFe_2O_4$	573	560
$Y_3Fe_5O_{12}$ (YIG)	560	195

[a] At T = 0(K).
Source: F. Keffer, *Handbuch der Physik*, vol. 18, pt. 2, Springer, New York, 1966.

Kittel

D. Gignoux, magnetic properties of Metallic systems

Antiferromagnetism

Negative exchange energy $J_{AB} < 0$.

↑↓↑↓↑↓↑↓

At low temperatures, below the Neel temperature T_N, the spins are aligned antiparallel and the macroscopic magnetization is zero.

Spin ordering can be observed by neutron scattering.

At high temperature antiferromagnets become paramagnetic. The macroscopic magnetization is zero and the spins are disordered in zero field.

$$\chi = \mu_0 \frac{\vec{M}_A + \vec{M}_B}{\vec{B}_a} = \frac{C}{T + \Theta}$$

Curie-Weiss temperature

Antiferromagnetism ↑↓↑↓↑↓↑↓

Average spontaneous magnetization is zero at all temperatures.

Source: Kittel

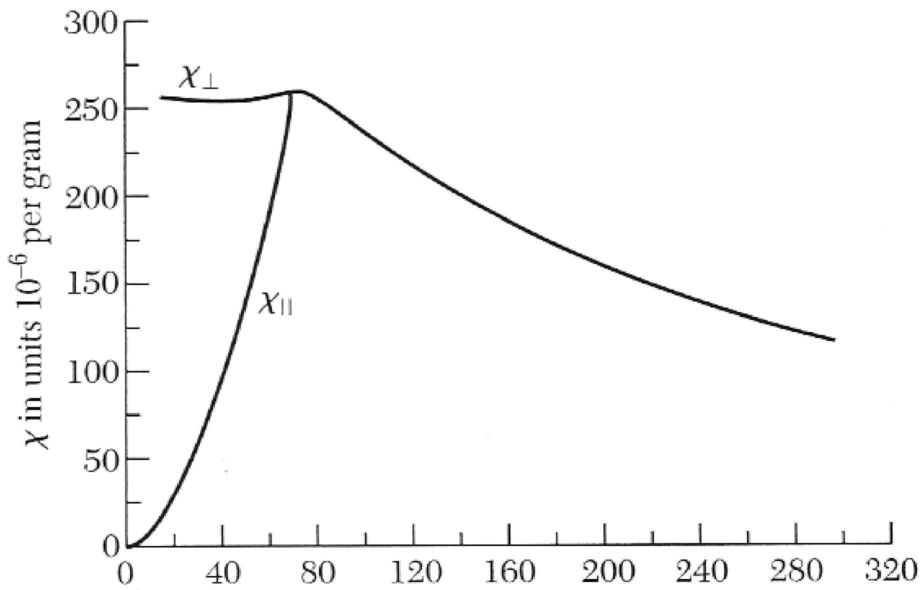

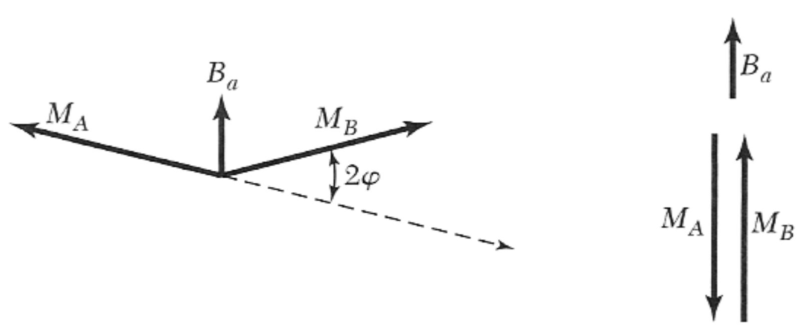

Table 2 Antiferromagnetic crystals

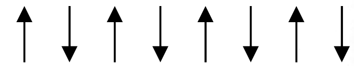

Substance	Paramagnetic ion lattice	Transition temperature, T_N, in K	Curie-Weiss θ, in K	$\frac{\theta}{T_N}$	$\frac{\chi(0)}{\chi(T_N)}$
MnO	fcc	116	610	5.3	$\frac{2}{3}$
MnS	fcc	160	528	3.3	0.82
MnTe	hex. layer	307	690	2.25	
MnF_2	bc tetr.	67	82	1.24	0.76
FeF_2	bc tetr.	79	117	1.48	0.72
$FeCl_2$	hex. layer	24	48	2.0	<0.2
FeO	fcc	198	570	2.9	0.8
$CoCl_2$	hex. layer	25	38.1	1.53	
CoO	fcc	291	330	1.14	
$NiCl_2$	hex. layer	50	68.2	1.37	
NiO	fcc	525	~2000	~4	
Cr	bcc	308			

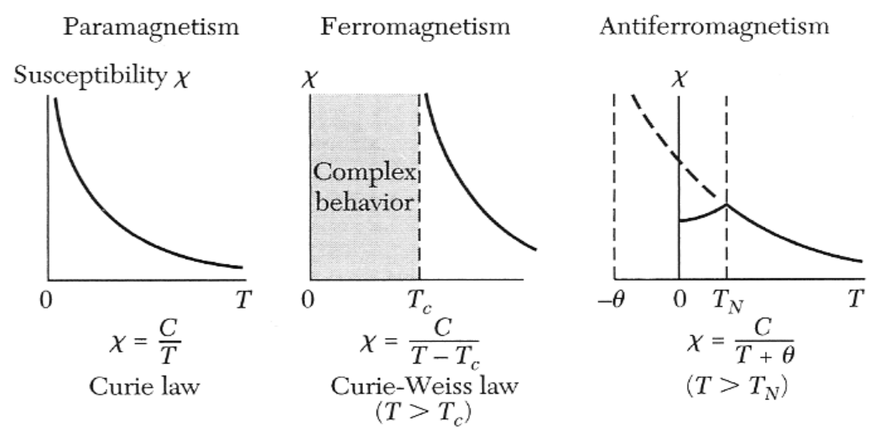

from Kittel

Applications of magnetism

Hard magnets: permanent magnets, motors, generators, microphones

Soft magnets: transformers

Magnetic recording

Magnetic domains (weisssche Bezirke)

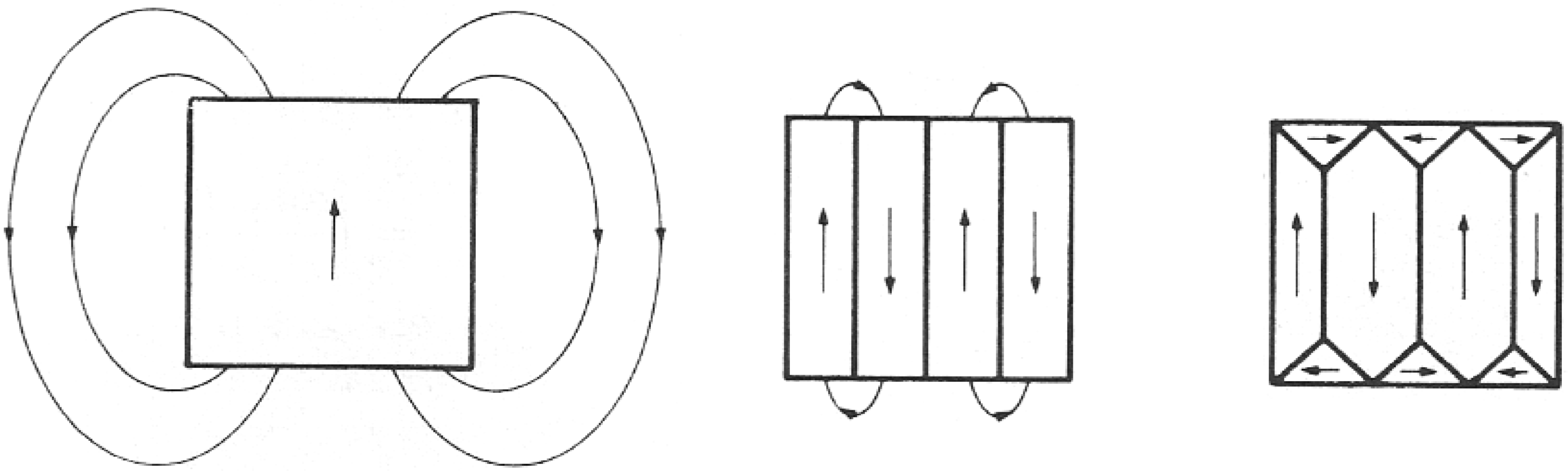

Magnetic energy density

$$\frac{B^2}{2\mu_0}$$

Costs energy to introduce domain walls where spin up regions are adjacent to spin down regions.

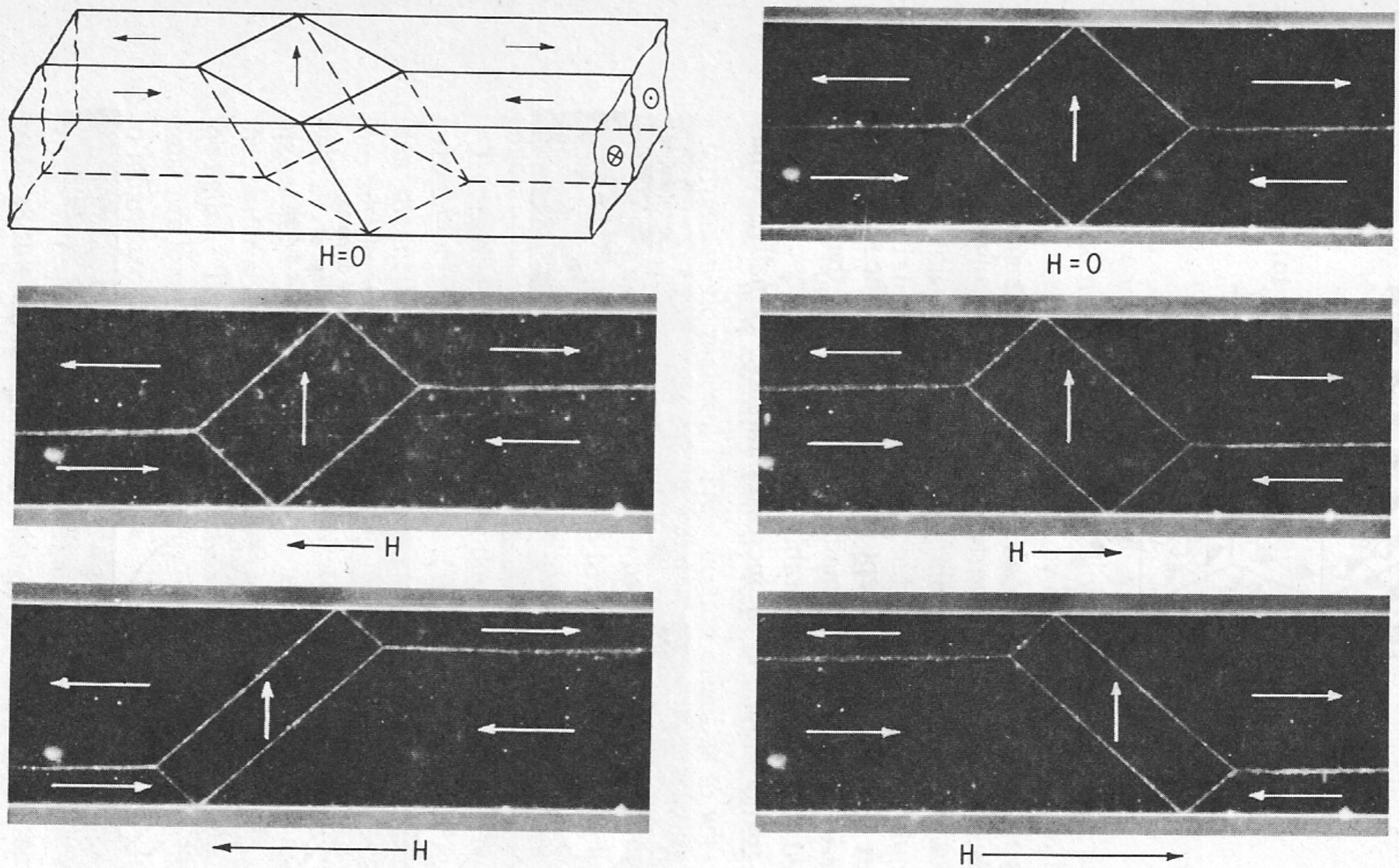
H=0
H=0
H
H
H
H

Ferromagnetic domains

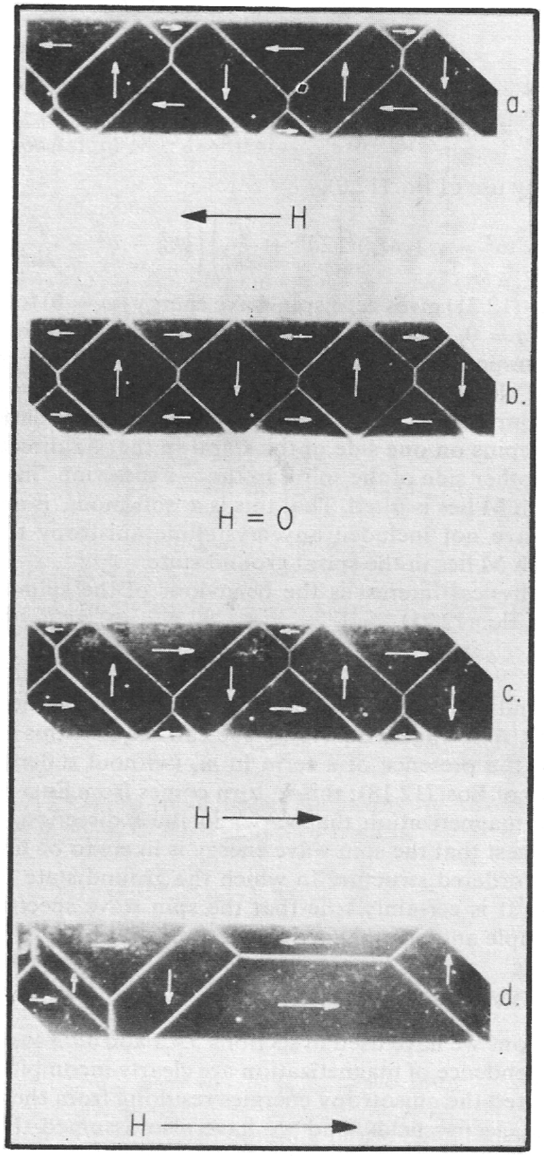

Fig. 12.5. Photographs showing reversible domain wall motion in a 50 μm whisker from (*a*) to (*b*) to (*c*), with an irreversible jump from (*c*) to (*d*).
{R. W. de Blois and C. D. Graham, *J. Appl. Phys.*, **29**, 931 (1958)}.

Weak fields: favorable domains expand
Strong fields: domains rotate to align with field

Irreproducible jump between c and d.

Magnetizing a magnet

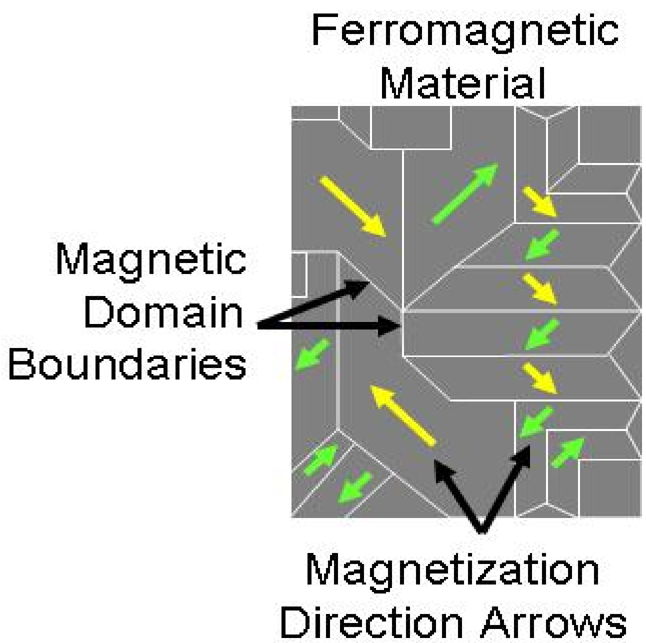

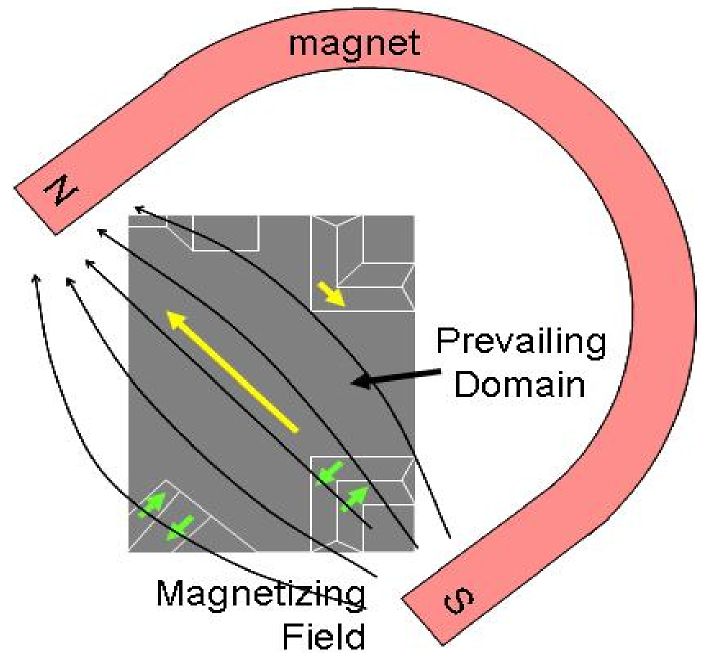

Weak fields: favorable domains expand
Strong fields: domains rotate to align with field

Hysteresis

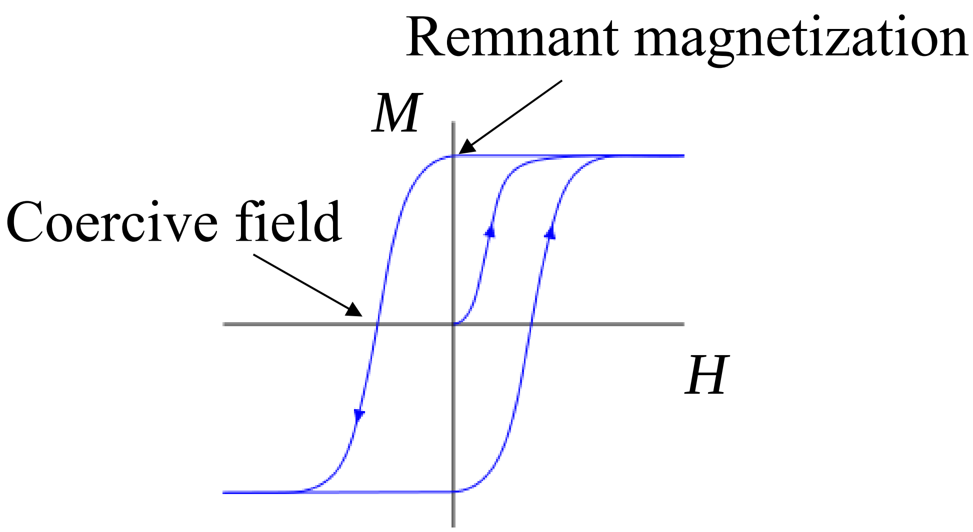

$$B = \mu_0 \left(H + M \right)$$

$$M = \chi H$$

$$B = \mu_0 (1 + \chi) H = \mu_r \mu_0 H$$

$$\mu_r = \left(1 + \chi \right)$$

Area of the loop is proportional to energy dissipated in traversing the loop.

Anisotropy energy

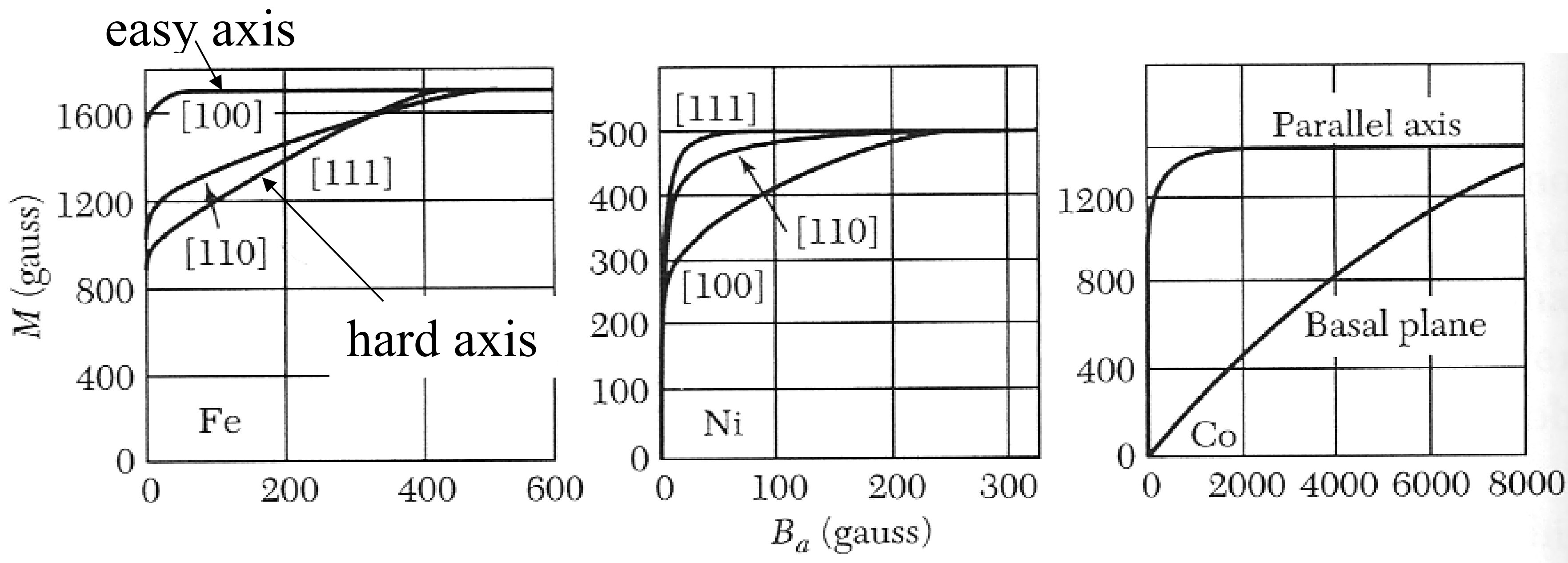

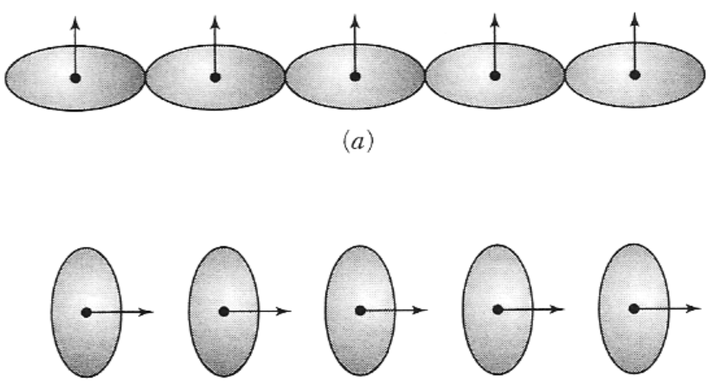

Spin-orbit coupling couples the shape of the wavefunction to the spin. The exchange energy depends on the overlap of the wavefunctions and thus on spin direction.

Bloch wall

energy of two spins

$$w = -J\vec{S}_i \cdot \vec{S}_j = -JS^2 \cos\varphi \approx -JS^2\left(1 - \frac{\varphi^2}{2}\right)$$

neglecting the constant part

$$w \approx JS^2 \frac{\varphi^2}{2}$$

$$\varphi = \frac{\pi}{N}$$

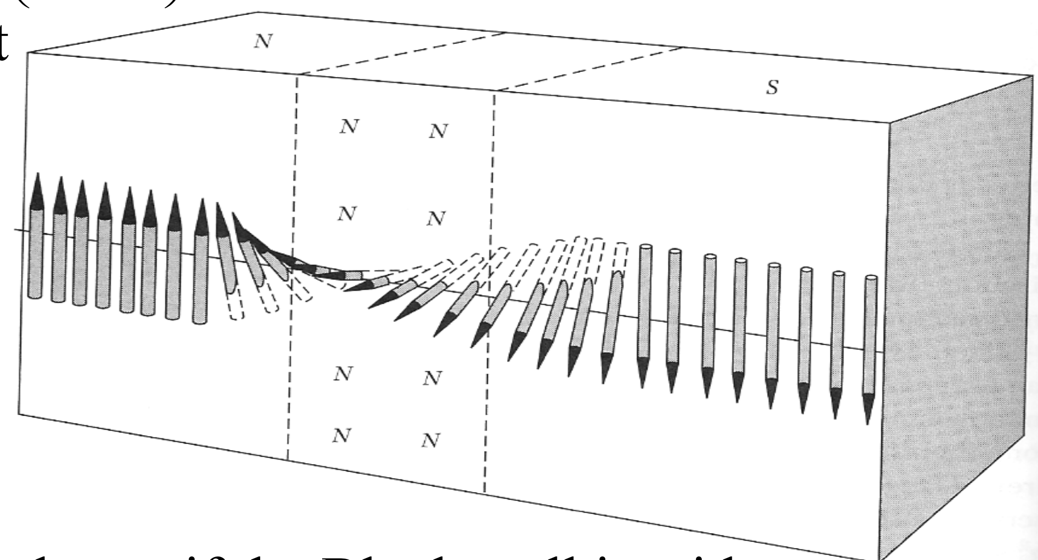

energy of a line of spins

$$Nw \approx \frac{JS^2\pi^2}{2N}$$

energy is lower if the Bloch wall is wide

energy per unit area $\approx \dfrac{JS^2\pi^2}{2Na^2}$

a is the lattice constant

Bloch wall

Anisotropy energy depends on the number of spins pointing in the hard direction

$\approx KNa$ ← Na = thickness of wall

↑ anisotropy constant J/m^3

Total energy per unit area:

$$E = \frac{JS^2\pi^2}{2Na^2} + KNa \quad [\mathrm{J/m^2}]$$

smaller for large N (first term) smaller for small N (second term)

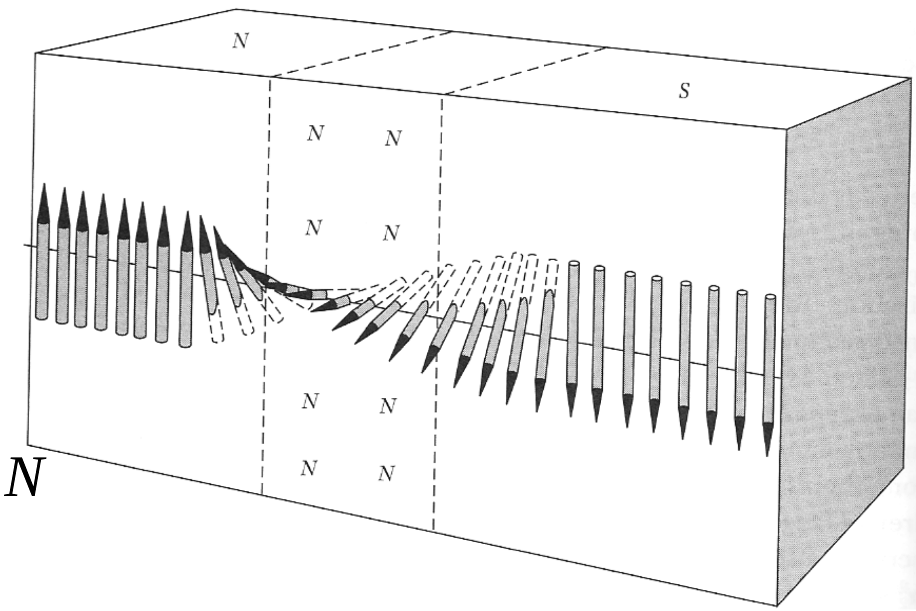

$$\frac{dE}{dN} = 0 \Rightarrow -\frac{JS^2\pi^2}{2N^2a^2} + Ka = 0$$

$$N = \sqrt{\frac{JS^2\pi^2}{2Ka^3}}$$

$N \sim 300$ for iron

Soft magnetic materials

soft magnets

MATERIAL	INITIAL RELATIVE PERMEABILITY (μ_r AT $B \sim 0$)	HYSTERESIS LOSS JOULE/m^3 PER CYCLE	B [T] SATURATION INDUCTION, WEBER/m^2
Commercial iron ingot	250	500	2.16
Fe-4% Si, random	500	50–150	1.95
Fe-3% Si, oriented	15,000	35–140	2.0
45 Permalloy (45% Ni-55% Fe)	2,700	120	1.6
Mumetal (75% Ni-5% Cu-2% Cr-18% Fe)	30,000	20	0.8
Supermalloy (79% Ni-15% Fe-5% Mo-0.5% Ma)	100,000	2	0.79

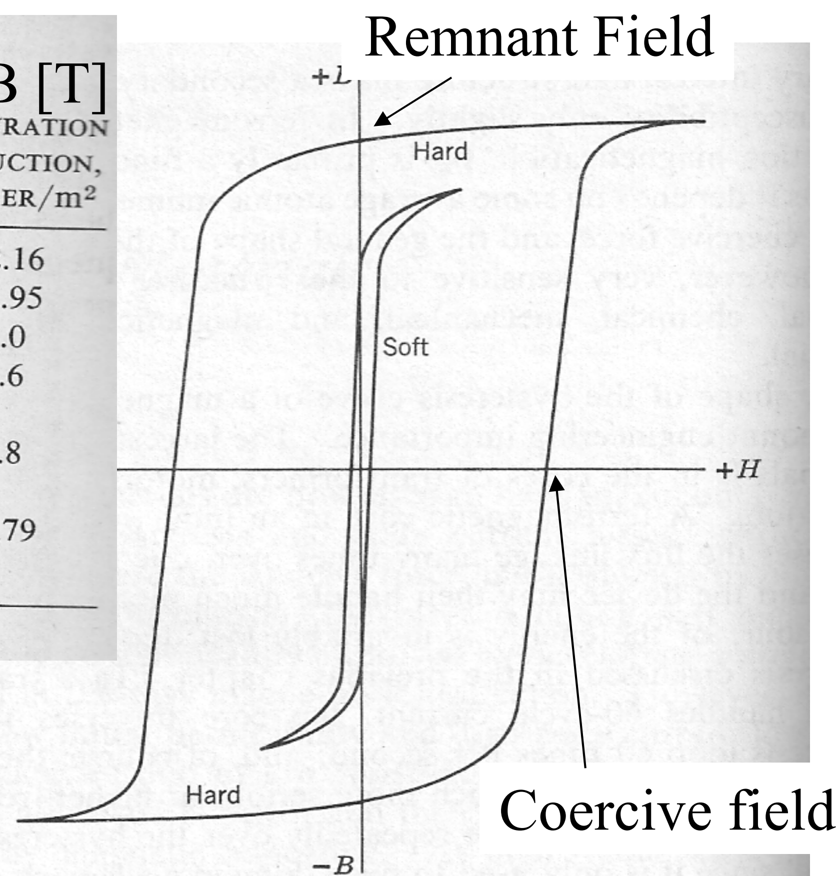

transformers
magnetic shielding
ferrites have low eddy current losses

$$B = \mu_0 \left(H + M \right)$$

$$B = \mu_r \mu_0 H$$

$$M = \chi H$$

$$\mu_r = 1 + \chi$$

Single domain particles

Small 10 - 100 nm particles have single domains.

Elongated particles have the magnetization along the long axis.

Single domains are used for magnetic recording. Long crystals can be magnetized in either of the two directions along the long axis.

Shape anisotropy.

Hard magnets

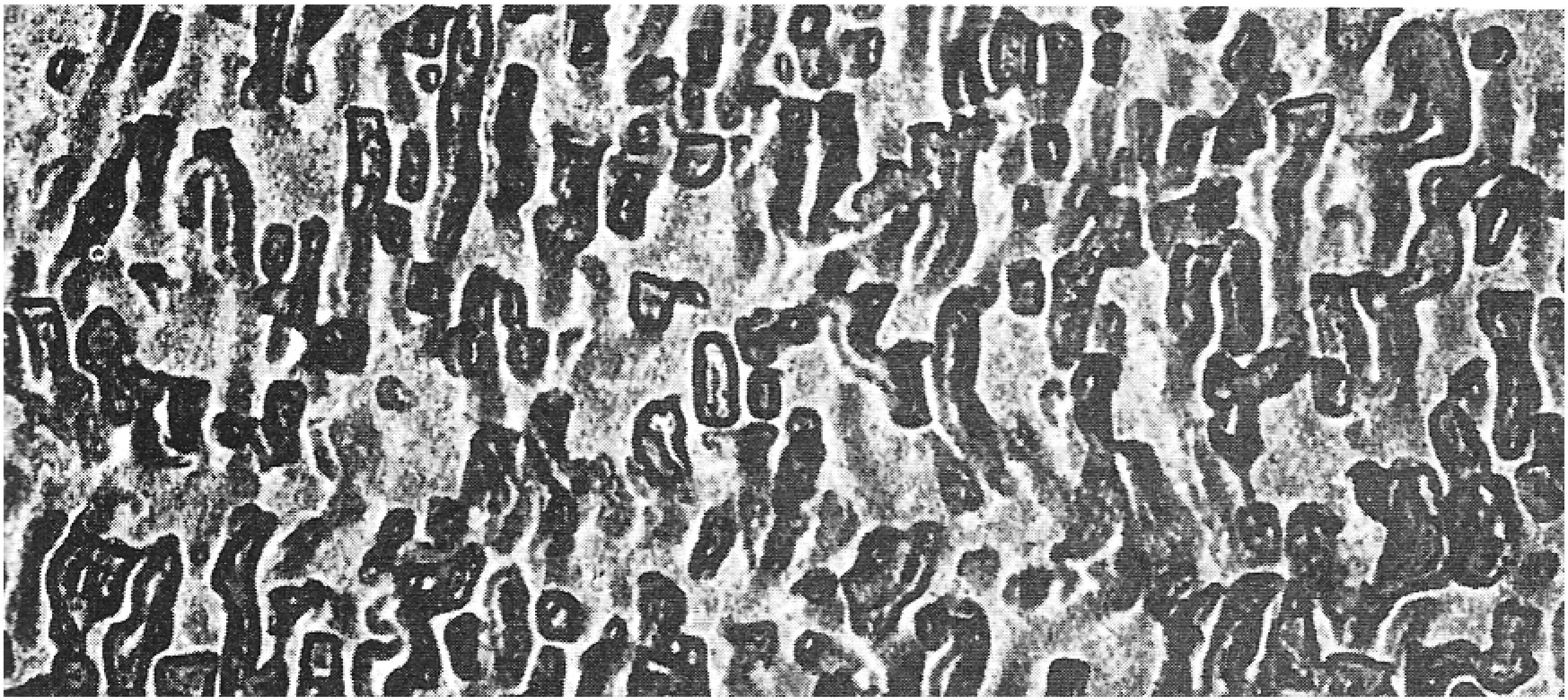

Grains too small to contain Bloch walls must be flipped entirely by the field.

Alnico: 8-12% Al, 15-26% Ni, 5-24% Co, up to 6% Cu, up to 1% Ti, rest is Fe

Hard magnetic materials

hard magnets

Magnet	B_r (T)	H_{ci} (kA/m)	$(BH)_{max}$ (kJ/m^3)	T_c (°C)
$Nd_2Fe_{14}B$ (sintered)	1.0–1.4	750–2000	200–440	310–400
$Nd_2Fe_{14}B$ (bonded)	0.6–0.7	600–1200	60–100	310–400
$SmCo_5$ (sintered)	0.8–1.1	600–2000	120–200	720
Sm(Co,Fe,Cu,Zr)$_7$ (sintered)	0.9–1.15	450–1300	150–240	800
Alnico (sintered)	0.6–1.4	275	10–88	700–860

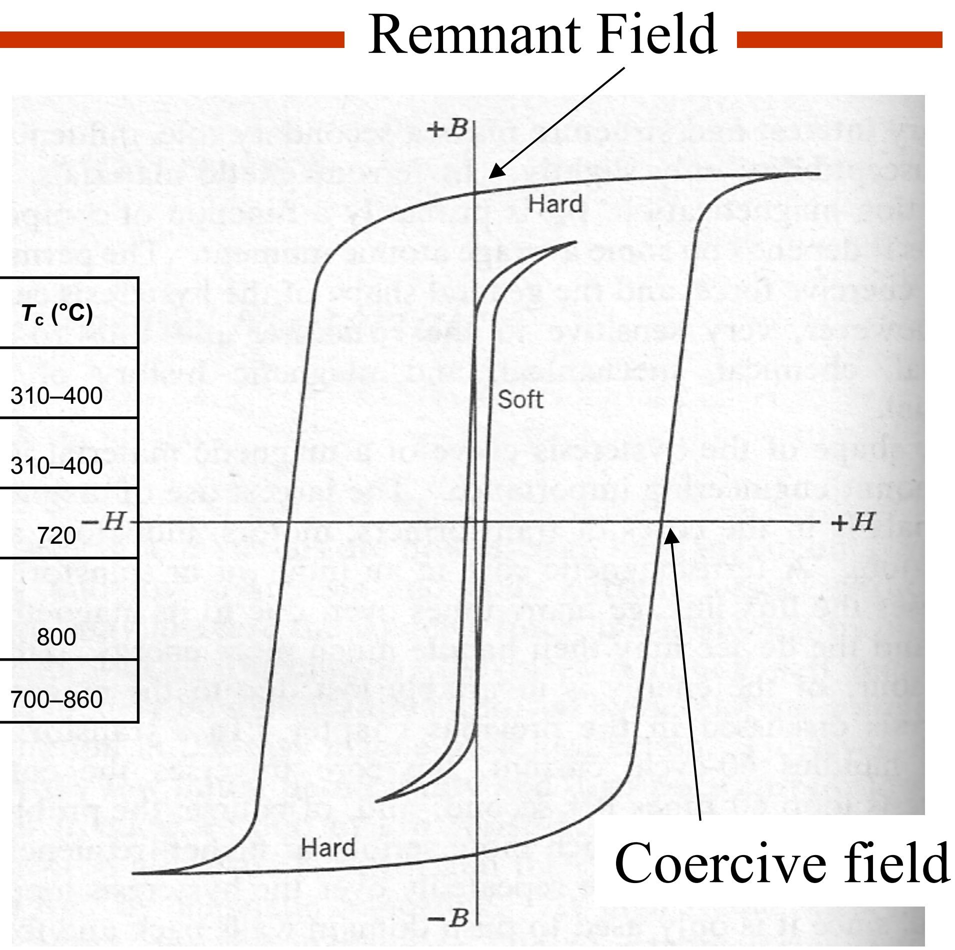

Permanent magnets, magnetron,
motors, generators
ferrites can also be hard magnets

Defects are introduced to pin the Bloch walls in a hard magnet.

Applications of hard magnets

Motors, generators, speakers, microphone

Superparamagnetism

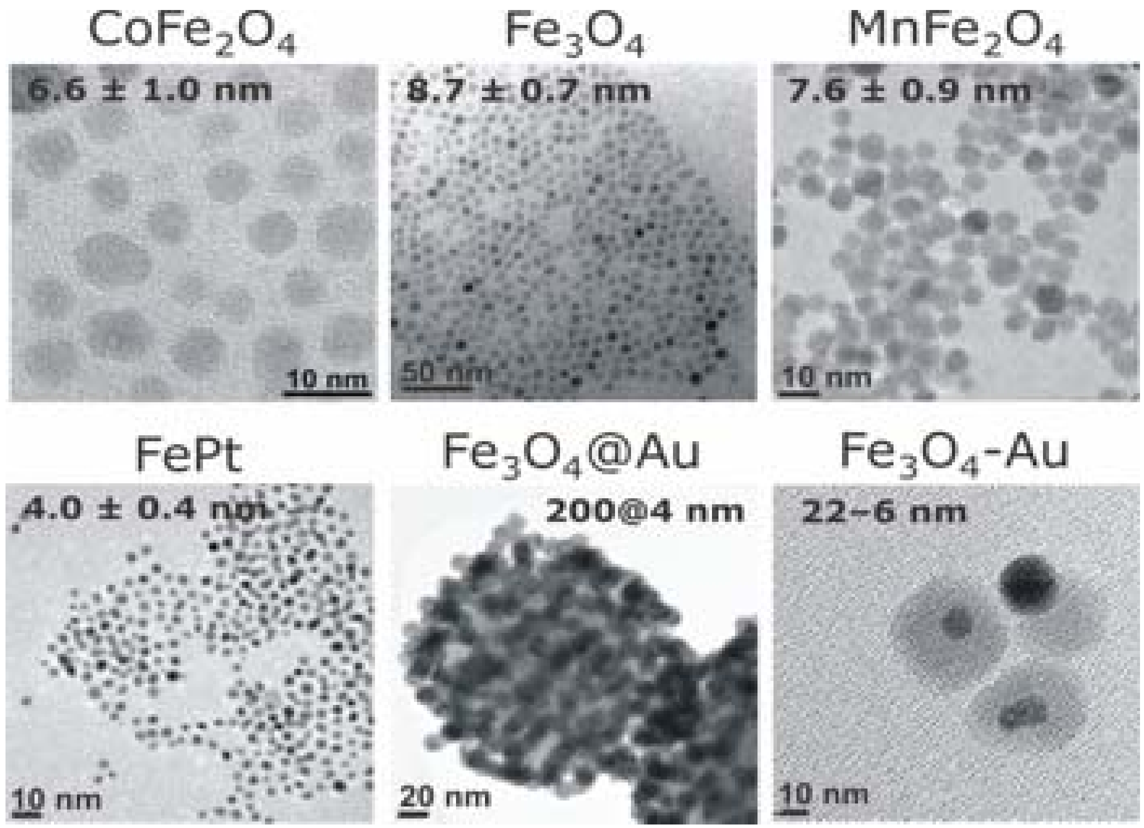

Below the Curie temperature the thermal energy changes the direction of magnetization of the entire crystallites.

http://www.imec.be/microsystems/bioelectronics/research/fn2.shtml

Composite magnets

Injection molded magnets are a composite of various types of resin and magnetic powders

Flexible magnets are made by embedding magnetic particles in vinyl.

Powers deposited on tapes for magnetic storage.

Magnetic tapes are much cheaper per GB than hard disks.

magnetic recording

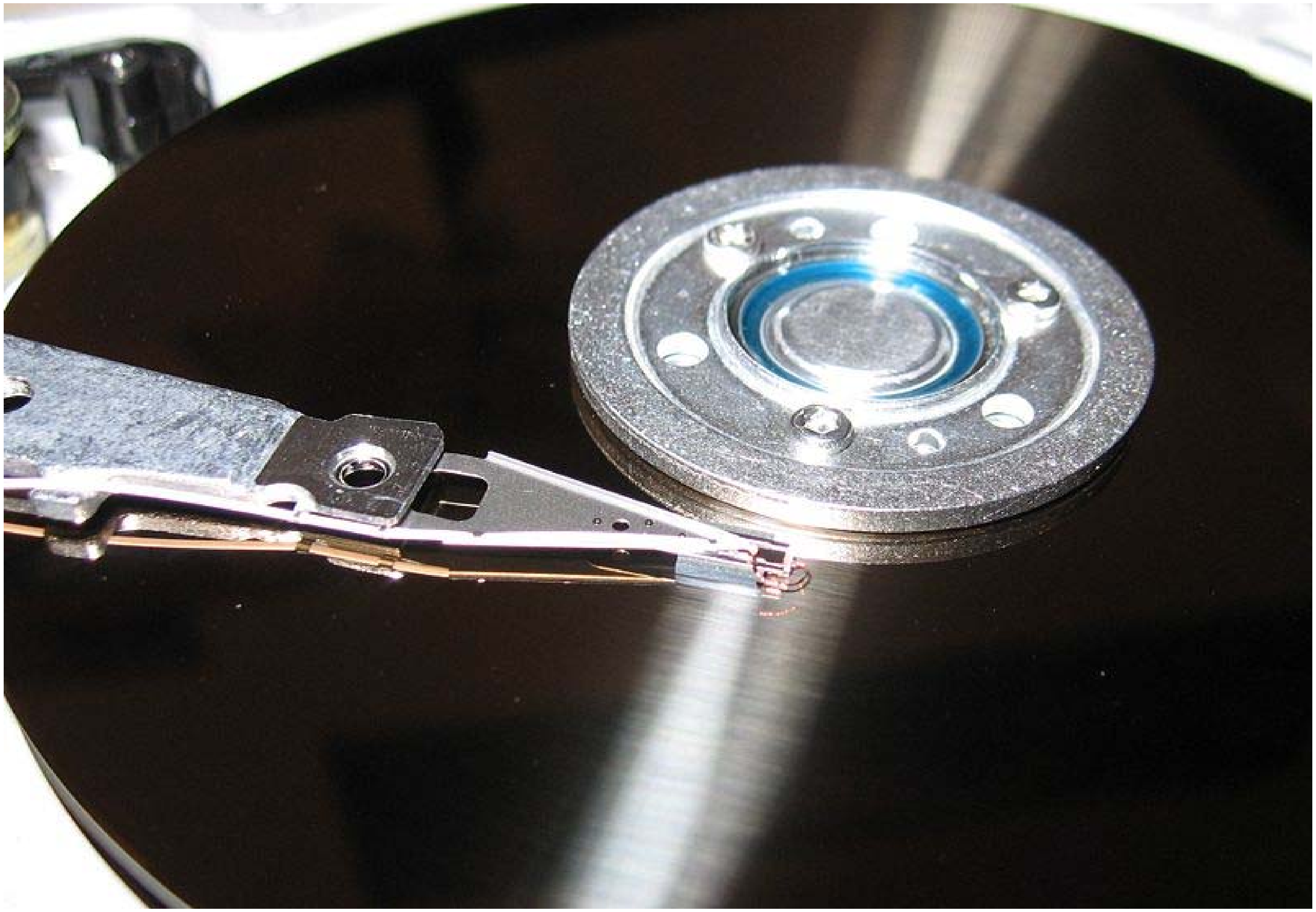

Giant magnetoresistance

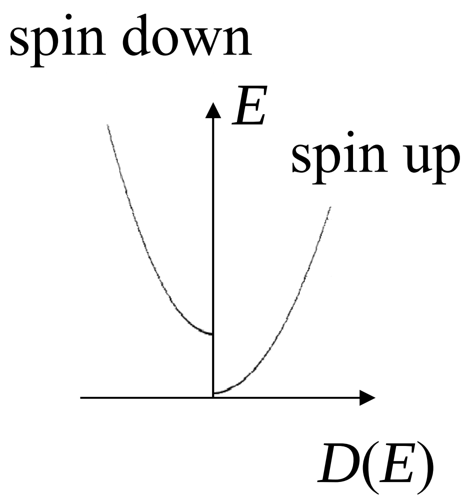

spin value

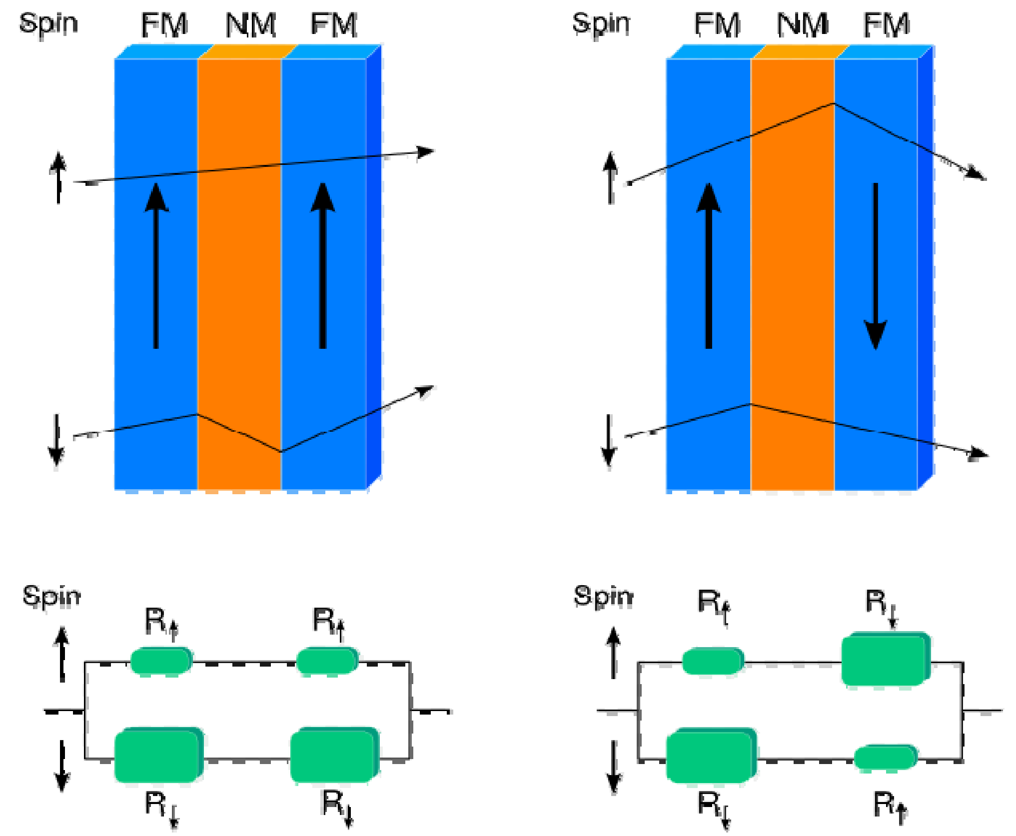

GMR sensors in read-heads for hard-disk drives

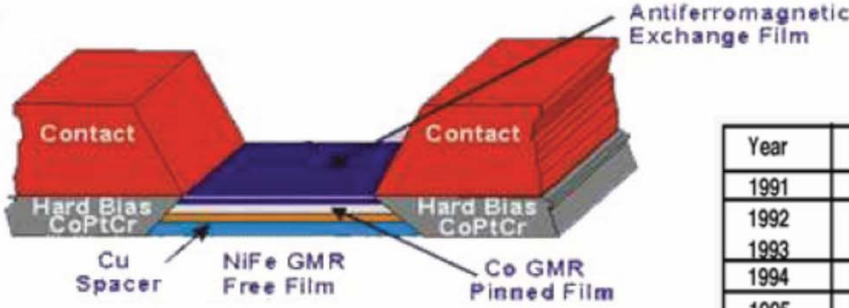

Shipment of GMR-read-heads (1997-2007):

5 billion (10^9)

Year	Areal Density Gbits/in2	Product
1991	0.132	Corsair
1992	0.260	Allicat
1993	0.354	Spitfire
1994	0.578	Ultrastar XP
1995	0.829	Ultrastar 2XP
	0.923	Travelstar 2LP
1996	1.32	Travelstar 2XP
	1.45	Travelstar VP
1997	2.64	Travelstar 5GS
	2.68	Deskstar 16GP
	3.12	Travelstar 6GN
1998	3.74	Travelstar 6GT
	4.1	Deskstar 25GP
	5.7	Travelstar 6GN
1999	5.3	Deskstar 37GP
	10.1	Travelstar 18GT
2000	7.04	Ultrastar 36LZX
	14.5	Deskstar 40GV
	17.1	Travelstar 30GT
2001	13.2	Ultrastar 73LZX
	25.7	Travelstarr 30GN
	29.7	Deskstar 120GXP
	34.0	Travelstar 40GN
2002	26.3	Ultrastar 146Z10
	45.5	Deskstar 180GXP
	29.7	Deskstar 120GXP
2003	70.0	Travelstar 80GN
2004	>100	
2005	>200	

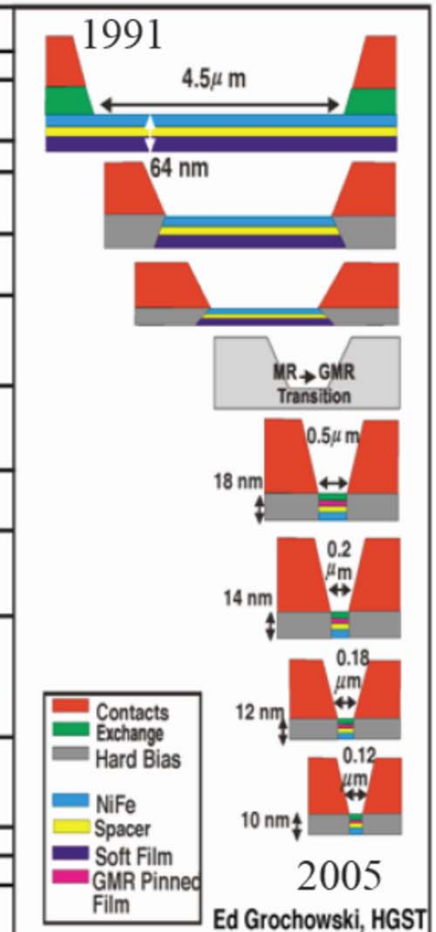

Peter Gruenberg Nobel Lecture 2007:

From Spinwaves to Giant Magnetoresistance (GMR) and Beyond

Magnetic force microscope

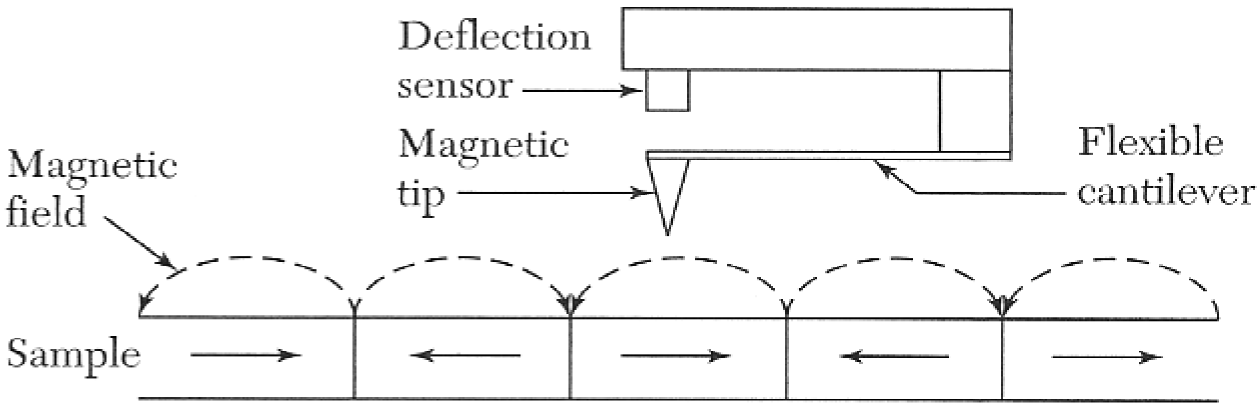

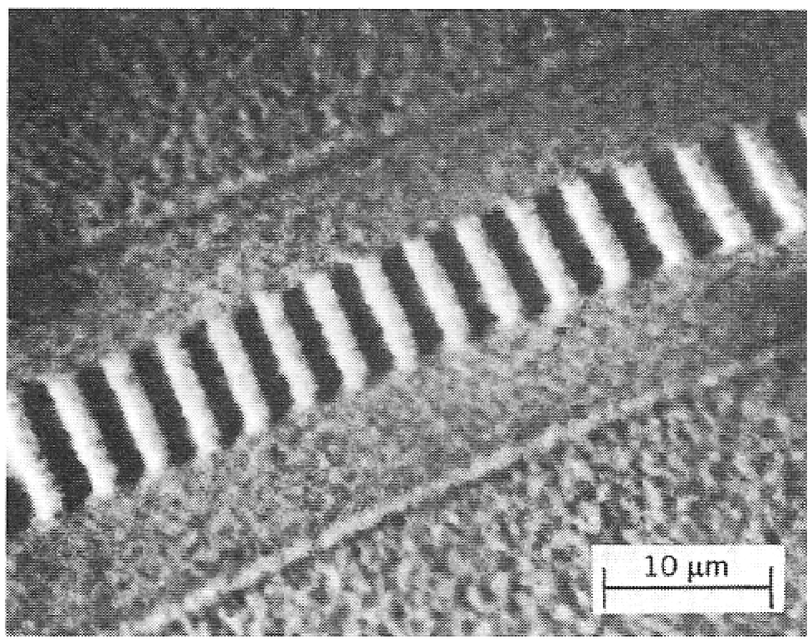

In-plane magnetization of a hard disk.